RASSF1A promotes apoptosis and suppresses the proliferation of ovarian cancer cells

LINGJIE FU and SHULAN ZHANG

Department of Gynaecology and Obstetrics, Shengjing Hospital of
China Medical University, Shenyang, Liaoning 110004, P.R. China

Abstract. As the most lethal gynecological malignancy, ovarian cancer has attracted much attention over the past few decades; however, the early detection of this malignancy has been largely unsuccessful. The aim of this study was to determine the effects of Ras-association domain family 1, isoform A (RASSF1A) on ovarian cancer and to elucidate the molecular mechanisms responsible for these effects. The expression of RASSF1A in different ovarian cancer cells was detected by quantitative reverse transcription-polymerase chain reaction (qRT-PCR). The morphology, structure, apoptosis and proliferation of differently treated SKOV-3 cells were then analyzed using a fluorescence microscope, transmission electron microscope, flow cytometer and by western blot analysis, respectively. Moreover, the GSE14407 affymetrix microarray data were downloaded from the Gene Expression Omnibus database and the expression of RASSF1A was quantified by Spotfire DecisionSite software. A RASSF1A related protein-protein interaction (PPI) network was then constructed using STRING and Cytoscape software. Finally, DAVID was utilized to perform KEGG pathway enrichment analysis of the network. RASSF1A was expressed in the HO8910, HO8910PM cells and the SKOV-3 cells transfected with RASSF1A, whereas it was absent in the other SKOV-3 cells and OVCAR-3 cells. Additionally, compared with the other SKOV-3 cells, the nucleus of SKOV-3 cells transfected with RASSF1A was vacuolated, apoptosis was increased, and the expression of cyclin D1 and survivin was decreased ($P<0.05$), and that of p27 and caspase-3 was increased ($P<0.01$). Additionally, 10 genes, including serine/threonine kinase (STK)3, STK4, Harvey rat sarcoma viral oncogene homolog (HRAS) and cell division cycle 20 (CDC20), were found to have close interactions with RASSF1A in the PPI network. Finally, a total of 8 enriched pathways, such as bladder cancer, non-small cell lung cancer and pathways in cancer were identified. To our knowledge, this is the first study to explore the biological functions and the underlying mechanisms of action of RASSF1A in the development of ovarian cancer. Our findings may provide a novel therapeutic target for ovarian cancer.

Introduction

Ovarian cancer is the leading cause of mortality from gynecological malignancies in the Western world, and the high case-fatality ratio associated with this malignancy may be attributed in part to its vague and non-specific symptoms (1). Although ovarian cancer confined to the ovaries has a 5-year survival of 92%, the majority of women with this type of cancer are diagnosed at an advanced stage (67%) and have a 5-year survival of only 30% (2). Due to the high mortality rate associated with ovarian cancer, a number of studies have been carried out in an attemtp to discover novel therapeutic approaches (3). Several biomarkers have been identified, such as human epididymis protein 4 (HE4) (4), transthyretin (5) and cancer antigen 125 (CA125) (6). However, these biomarkers are not sufficient for the early diagnosis of ovarian cancer. Therefore, there is an urgent need to discover novel therapeutic targets and to explore their molecular mechanisms of action in ovarian cancer.

Ras-association domain family 1, isoform A (RASSF1A) is a tumor suppressor gene which is usually inactivated in human cancers (7). Donninger *et al* (8) discovered that RASSF1A is pro-apoptotic and may serve to integrate pro-growth and pro-death signaling pathways. Kassler *et al* (9) observed a strong correlation between RASSF1A expression and the development of resistance to Taxol in ovarian cancer. In addition, RASSF1A has been shown to be closely associated with the progression of prostate (10), thyroid (11), blood-based breast (12) and primary non-small cell lung cancer (13). Furthermore, RASSF1A has been shown to suppress melanoma development by encoding a microtubule-associated protein which may regulate cell proliferation, migration and apoptosis (14). Besides, RASSF1A interacts with effectors of apoptotic pathways, including macrophage stimulating protein (MST)1/2 and modulator of apoptosis 1 (MOAP1), resulting in the induction of apoptosis (15). It has been demonstrated

Correspondence to: Dr Shulan Zhang, Department of Gynaecology and Obstetrics, Shengjing Hospital of China Medical University, 36 Sanhao Street, Shenyang, Liaoning 110004, P.R. China
E-mail: shulanzhang001fh@hotmail.com

that RASSF1A expression inhibits the tumorigenic potential of A375 cells in nude mice, which correlates with decreased cell proliferation and increased apoptosis (14). It has also been reported that RASSF1A suppresses melanoma development by modulating apoptosis and cell cycle progression (14); however, the underlying mechanisms have not yet been elucidated. Thus, RASSF1A possesses great potential as a therapeutic target in human cancer.

Furthermore, the development of computational tools and resources for genetic analysis has accelerated rapidly over the past decades (16). A number of researchers have utilized bioinformatics approaches to explore the molecular mechanisms of diseases and have discovered novel biomarkers (17,18). In this study, the expression of RASSF1A in 4 ovarian cancer cell lines and in differently treated SKOV-3 cells was detected. The effects of RASSF1A on cell morphology, structure, apoptosis and proliferation were also examined. Moreover, the mechanisms responsible for these effects were explored using a bioinformatics approach. Our data suggest that RASSF1A is a novel biomarker for ovarian cancer and may aid in the early detection, prevention and treatment of the disease.

Materials and methods

Ovarian tumor tissuses and cell line collection. A total of 47 patients with malignant ovarian epithelial tumors (43 serous cystadenocarcinoma cases and 4 borderline cases), who underwent surgery (one-time treatment) at the hospital of China Medical University Graduate School from September 2005 to January 2008, were recruited for sample collection. Among these 47 cases, 5 cases were at clinical stage I, 4 cases at stage II, 37 cases at stage III and 1 case at stage IV. Ovarian samples from 10 patients who underwent an ovarian anatomical examination or prophylactic ovariotomy were collected as control group. All the ovarian samples were collected under sterile conditions and pathologically validated. After being excised from the human body, the ovarian samples were quickly frozen in liquid nitrogen and transferred to -80°C freezer. The ovarian epithelial cancer cells (HO8910, HO8910PM, SKOV-3 and OVCAR-3) were purchased from the Cell Bank of the Chinese Academy of Sciences.

All patients provided written informed consent, and the Ethics Committee of China Medical University Graduate School (Shenyang, China) approved all aspects of this study.

Quantitative reverse transcription-polymerase chain reaction (qRT-PCR). Total RNA was extracted from the samples using TRIzol reagent (Invitrogen, Carlsbad, CA, USA), and the protocol was performed according to the manual provided by the manufacturer. cDNA was synthesized from 2 μg of total RNA in a 10-μl reaction system containing 2 μl MgCl$_2$, 1 μl 10X RT buffer, 3.75 μl RNase-Free H$_2$O, 1 μl dNTP mixture (10 mM), RNase inhibitor 0.25 μl, AMV reverse transcriptase 0.5 μl, random 9 mers 0.5 μl and RNA 1 μl.

The primers for RASSF1A and β-actin were designed as follows and synthetized by Saibaisheng Biological Engineering Co., Ltd., Beijing, China: RASSF1A forward, 5'-CTTCATCT GGGGCGTCGTG-3' and reverse, 5'-GCATCCTTGGGCA GGTAAAA-3'. The target fragment length for RASSF1A was 420 bp. The primers for β-actin were as follows: forward,

5'-TGCGTGACATTAAGGAGAAGC-3' and reverse, 5'-GAA GGTGGACAGCGAGGC-3'. The target fragment length for β-actin was 431 bp.

PCR was carried out according using the Takara RNA PCR kit version 3.00 (Takara Bio, Dalian, China) in a 20-μl reaction volume (cDNA template 4 μl, 5X PCR buffer 4 μl, distilled water 7.9 μl, Ex Taq Hot Start (HS) 0.1 μl, sense primer 2 μl and reverse primer 2 μl) with the following protocol: 94°C for 30 sec, 57°C for 30 sec and 72°C for 40 sec for 30 cycles. All the PCR reactions were conducted using a Biometra PCR system (Biometra, Göttingen, Germany). PCR products were separated on 1.5% Tris-borate EDTA agarose gels with a100-bp DNA Ladder Marker (Dalian Bao Biological Engineering Co., Dalian, China), hybridized and visualized using an electrophoresis gel imaging system (ChemiImager 5500; Alpha Innotech, San Leandro, CA, USA).

Transfection in vitro. The SKOV-3 cells were cultured in medium which contained 100 U/ml penicillin, 100 μg/ml streptomycin and 10% fetal bovine serum (FBS) (Sigma-Aldrich, St. Louis, MO, USA) in a humidified atmosphere of 5% CO$_2$. The exponential cells were then collected and seeded on a 6-well cell culture cluster at a concentration of 5x10^5 cells/well and allowed to grow overnight. When grown to 85-90%, the SKOV-3 cells were transfected with green fluorescent protein (GFP)-labeled adenovirus with or without RASSF1A (Baisai Biological Co., Beijing, China). Untransfected SKOV-3 cells were used as controls.

Quantification of RASSF1A expression in SKOV-3 cells. The SKOV-3 cells were collected after 24-48 h of transfection, and the differential expression of RASSF1A was detected by qRT-PCR. The protocol of RT-PCR was similar to the one described above.

Analysis of cell morphology, structure and apoptosis. A fluorescence microscope (BX5O; Olympus, Tokyo, Japan) was used to analyze the morphology of the SKOV-3 cells following transfection and observe the location of fluorescence. A transmission electron microscope (TEM; JEM 1010, Jeol, Tokyo, Japan) was then used to observe the structure of the transfected and untransfected SKOV-3 cells. Furthermore, a flow cytometer (TOA Medical Electronics Co., Ltd., Kobe, Japan) was utilized to analyze the cycle and apoptosis of SKOV-3 cells treated with adenovirus with or without RASSF1A. The protocol involved digestion with 0.25% pancreatin, washing with phosphate-buffered saline (PBS) buffer, fixation with 70% ethanol at 20°C for 10 h, and dying with propidium iodide for 30 min. The cells, including SKOV-3 cells transfected with adenovirus with or without RASSF1A and untransfected SKOV-3 cells were analyzed by flow cytometry using an Apoptosis detection kit (KGI Biotechnology Development Co., Ltd., Nanjing, China). Each group had 10 duplications and the results were analyzed using multifunctional software systems.

Preparation and quantification of protein expression. The SKOV-3 cells, including untreated cells, and those transfected with adenovirus with or without RASSF1A, were cultured in 6-well plates and each type of cell was allocated 2 wells. The cells were washed with 1X PBS buffer (pH 7.4) 3 times and

digested by 0.25% pancreatin. Pancreatin was removed by centrifugation at 2,000 rpm for 5 min (high-speed refrigerated centrifuge 31K5C; Sigma-Aldrich) followed by the addition of 100 μl RIPA buffer which contained 1X PBS buffer, 1% NP-40, 0.5% sodium deoxycholate, 0.1% sodium dodecyl sulfate (SDS) and protease inhibitor, such as phenylmethylsulfonyl fluoride (PMSF; Takara Bio). Following ultrasonic dispersion for 30 sec, the samples were incubated on ice for 30 min. The supernatant was transferred to a new tube after centrifugation at 10,000 x g for 10 min at 4°C (high-speed refrigerated centrifuge 31K5C; Sigma-Aldrich) and then the centrifugation was repeated once. In addition, the proteins were quantified using the Bradford method, as previously described (19).

Western blot analysis. The protein samples were separated by sodium dodecyl sulfate-polyacrylamide gel electrophoresis (SDS-PAGE) followed by transfer onto polyvinylidene fluoride (PVDF) membranes (Millipore, Billerica, MA, USA). The PVDF membranes were then blocked overnight with 0.1% Tween-20, 1X PBS and 5% non-fat milk. The membranes were then washed with buffer containing 0.1% Tween-20 and 1X PBS for 5 min. Following incubation with rabbit anti-human Livin antibody (1:400; Imgenex Corp, San Diego, CA, USA) or antibodies against cyclin D1, survivin, p27, caspase-3 and GAPDH (Wuhan Boshide Bioengineering Co., Ltd., Wuhan, China) for 2 h at room temperature, the membranes were hybridized with goat anti-rabbit antibodies (Zhongshan Golden Bridge Biotechnology Co., Beijing, China) for 1 h and washed with 0.1% Tween-20 and 1X PBS 3 times for 5 min each. The membranes were subsequently treated with alkaline phosphatase for 5-30 min and the results were analyzed using Scion Image software (Scion Corp., Frederick, MD, USA) by calculating the target protein/GAPDH ratio, as previously described (20).

Statistical analysis. Statistical analysis was carried out using SPSS 12.0 software. P-values <0.05 and <0.01 were considered to idicate statistically significant and highly statistically significant differences, respectively.

Derivation of genetic data. The gene expression profile data of GSE14407 (21) was downloaded from a public functional genomics data repository, the Gene Expression Omnibus (GEO, http://www.ncbi.nlm.nih.gov/geo/) database. A total of 24 specimens, including 12 healthy ovarian surface epithelial samples (OSE) and 12 laser capture microdissected serous ovarian cancer epithelial samples (CEPI), were available based on the Affymetrix 3' expression array.

Detection of the expression of RASSF1A. The derived genetic data were analyzed using Spotfire DecisionSite software (http://spotfire.tibco.com; TIBCO Software Inc., Palo Alto, CA, USA) (22). The differentially expressed genes (DEGs) were identified with a fold change value >3 and a value of P<0.05 (Student's t-test). Furthermore, we detected whether RASSF1A was in the list of DEGs.

Construction of protein-protein interaction (PPI) network. The online database resource Search Tool for the Retrieval of Interacting Genes (STRING) provides uniquely compre-
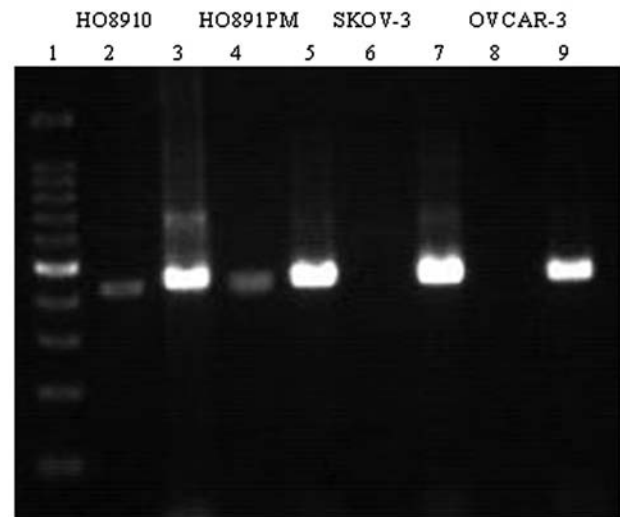

Figure 1. mRNA expression of Ras-association domain family 1, isoform A (RASSF1A) in different ovarian cancer cell lines. Lane 1 represents the DNA marker; lanes 2, 4, 6 and 8 represent RASSF1A bands, while lanes 3, 5, 7 and 9 represent β-actin bands.

hensive coverage and ease of access to both experimental and predicted interaction information (23). In the present study, the interactions between RASSF1A and other genes were derived based on STRING and the associations with a correlation coefficient >0.4 were identified as PPIs. The PPI network was constructed and visualized using Cytoscape software, as previously described (24). Cytoscape is an open source software project for integrating biomolecular interaction networks with high-throughput expression data and other molecular states into a unified conceptual framework.

Pathway enrichment analysis. The Database for Annotation, Visualization and Integrated Discovery (DAVID) contains an integrated biological knowledge base and analytic tools, aiming at systematically extracting biological meaning from large gene/protein lists (25). The Kyoto Encyclopedia of Genes and Genomes (KEGG) is a knowledge base for the systematic analysis of gene functions, linking genomic information with higher order functional information (26). In this study, pathway enrichment analysis was performed for the PPI network by DAVID and the significantly enriched pathways were identified with a value of P<0.05.

Results

Expression of RASSF1A. RASSF1A mRNA was expressed in the HO8910 and HO8910PM cells and was absent in the SKOV-3 and OVCAR-3 cells (Fig. 1). RASSF1A mRNA expression was detected in all 10 normal ovarian tissues (100%), while RASSF1A mRNA was detected in 2 cases among the 47 ovarian tumor samples (4.3%). The expression of RASSF1A in the differently treated SKOV-3 cells was detected by qRT-PCR; no RASSF1A expressoin was detected in the SKOV-3 cells transfected with adenovirus without RASSF1A (Fig. 2). However, high expression levels of the RASSF1A gene were found in the SKOV-3 cells transfected with adenovirus carrying RASSF1A.

Table I. Protein-protein interactions and their combined scores.

| Node 1	Node 2	Combined score	Node 1	Node 2	Combined score
MDM2	UBC	0.999	RASSF1	SAV1	0.956
MDM2	CDKN2A	0.999	RASSF1	E4F1	0.953
STK3	SAV1	0.997	RASSF1	UBC	0.95
STK4	SAV1	0.996	CDKN2A	RASSF1	0.947
STK4	RASSF1	0.996	CDKN2A	E4F1	0.94
RASSF1	HRAS	0.993	MDM2	HRAS	0.923
RASSF1	CDC20	0.991	STK3	STK4	0.9
STK3	RASSF1	0.985	UBC	HRAS	0.858
RASSF1	MOAP1	0.976	CDKN2A	HRAS	0.752
UBC	CDC20	0.975	UBC	MOAP1	0.507
MDM2	RASSF1	0.974	STK3	MOAP1	0.502
CDKN2A	UBC	0.961	E4F1	MOAP1	0.401
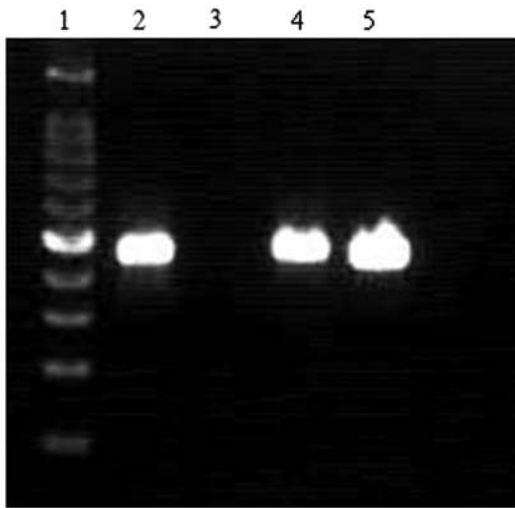
Figure 2. Expression of Ras-association domain family 1, isoform A (RASSF1A) in different SKOV-3 cells. Lane 1 represents the DNA marker; lanes 3 and 5 represent RASSF1A bands, while lanes 2 and 4 represents β-actin bands. Lanes 2 and 3 represent SKOV-3 cells transfected with adenovirus without RASSF1A, while lanes 4 and 5 represent cells transfected with green fluorescent protein (GFP)-labeled adenovirus carrying RASSF1A.

Morphology and structure of SKOV-3 cells. The morphology of the transfected and untransfected SKOV-3 cells was examined under fluorescence microscope after 24 h of transfection. The untreated SKOV-3 cells showed the stripping away of the cell wall and had projections on their surface (Fig. 3A). However, the transfected cells were round in shape and the volumes were increased; the nucleus was vacuolated (Fig. 3B). In addition, the fluorescence location in the transfected SKOV-3 cells was observed after 48 h of treatment. Fluorescent aggregates were observed in the cytoplasm and were mainly distributed in the cytoskeleton (Fig. 3C). Moreover, a TEM was utilized to study the structure of the SKOV-3 cells. The untransfected cells showed a regular growth (Fig. 3D), whereas the nuclear chromatin of the transfected cells displayed obvious shrinkage, condensation and apoptotic bodies had formed (Fig. 3E).

Analysis of apoptosis. With the use of a flow cytometer and an apoptosis detection kit, the cycle and apoptosis of SKOV-3 cells (untreated cells and cells transfected with adenovirus with or without RASSF1A) were analyzed (Fig. 4). In the S phase of the cell cycle, a significantly greater number of transfected SKOV-3 cells (cells transfected with adenovirus with or without RASSF1A) was observed, compared with the untreated cells (P<0.05). Furthermore, the rate of apoptosis of the SKOV-3 cells transfected with RASSF1A was significantly greater than that of the other cells (untreated cells and those transfected with adenovirus without RASSF1A) (P<0.01).

Results of western blot analysis. The expression of cyclin D1 and survivin in the SKOV-3 cells transfected with adenovirus carrying RASSF1A was decreased significantly compared with the untreated cells and those transfected with adenovirus without RASSF1A (P<0.05). However, the expression of p27 and caspase-3 in the SKOV-3 cells transfected with RASSF1A was increased highly significantly compared with the other SKOV-3 cells (untreated cells and those transfected with adenovirus without RASSF1A) (P<0.01) (Fig. 5).

PPI network. The GSE14407 gene expression data were analyzed and the DEGs between the OSE and CEPI samples were identified. However, the RASSF1A gene was discovered not to be in the list of DEGs in our study. Based on STRING and Cytoscape software, a RASSF1A-related PPI network was constructed (Fig. 6). In this network, a total of 10 genes, including serine/threonine kinase (STK)4, Harvey rat sarcoma viral oncogene homolog (HRAS), cell division cycle 20 (CDC20), STK3, modulator of apoptosis 1 (MOAP1), salvador homolog 1 (*Drosophila*) (SAV1), E4F1, ubiquitin C (UBC), murine double minute 2 (MDM2) and DKN2A was found to be closely associated with RASSF1A (Table I).

Pathway enrichment analysis. KEGG pathway analysis was conducted using DAVID and a total of 8 pathways were identified with values of P<0.05 (Table II). The RASSF1A gene was shown to participate in 3 significant pathways, including bladder cancer (P=1.79E-05), non-small cell lung cancer
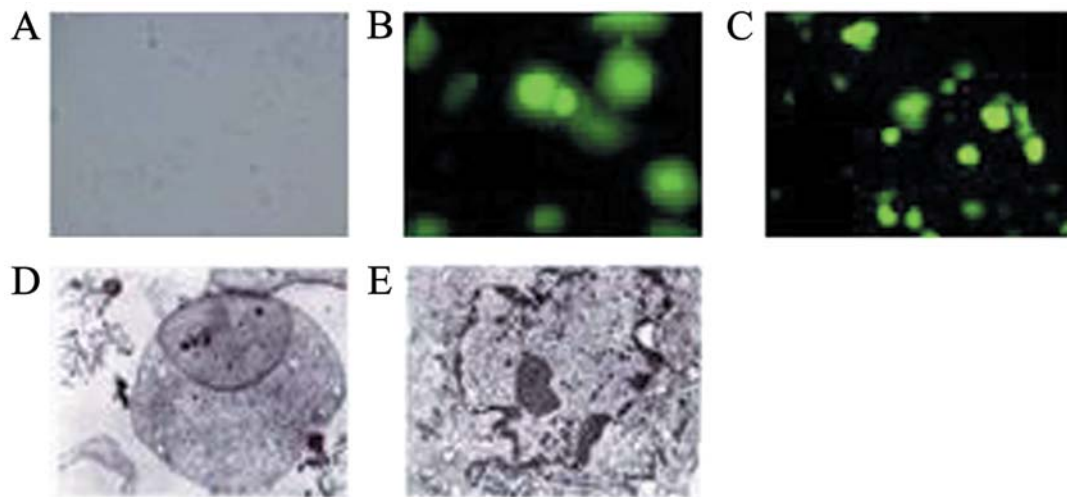
Figure 3. Morphology and structure observation of SKOV-3 cells. (A and D) Untransfected SKOV-3 cells. (B and E) SKOV-3 cells transfected with adenovirus carrying Ras-association domain family 1, isoform A (RASSF1A). (C) Fluorescence distribution in SKOV-3 cells. (A-C) Morphology of SKOV-3 cells. (D and E) Structure of SKOV-3 cells.
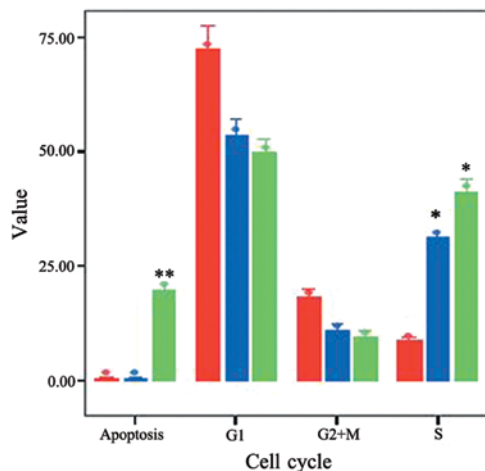

Figure 4. Apoptosis of SKOV-3 cells. Red bars indicate untransfected SKOV-3 cells, blue bars represent the cells transfected without Ras-association domain family 1, isoform A (RASSF1A) and the green bars represent the SKOV-3 cells transfected with adenovirus carrying RASSF1A.

(P=3.85E-05) and pathways in cancer (P=5.09E-04). In addition, all the enriched pathways were associated with cancer.

Discussion

In spite of great efforts that have been made by researchers to enable the early diagnosis of ovarian cancer, the results have not been satisfactory and the pathogenesis of the disease is not yet fully understood (27). In this study, the RASSF1A gene was found to be present in HO8910 and HO8910PM cells, and absent in SKOV-3 and OVCAR-3 cells. The SKOV-3 cells were then transfected by an adenovirus with or without RASSF1A, and RASSF1A expression in the differently treated SKOV-3 cells was analyzed by qRT-PCR. Moreover, the morphology and structure, as well as the apoptotic and proliferative ability of the SKOV-3 cells transfected with adenovirus carrying RASSF1A were altered significantly compared with the untreated SKOV-3

cells. Furthermore, the RASSF1A gene was shown to induce apoptosis and suppress cell proliferation through several cancer-related pathways by interacting with other genes.

Firstly, the expression of RASSF1A in 4 types of human ovarian cancer cell lines, including HO8910, HO8910PM, SKOV-3 and OVCAR-3, was detected by qRT-PCR. The result revealed that RASSF1A is absent in SKOV-3 and OVCAR-3 cells, while it is present in the HO8910 and HO8910PM cells. Our findings are consistent with those of a previous study showing that SKOV-3 and OVCAR-3 cells represent an ovarian cancer, referred to as serous adenocarcinoma (28). We subsequently transfected SKOV-3 cells with an adenovirus with or without RASSF1A and the expression of RASSF1A in the differently treated SKOV-3 cells was analyzed. The expression of RASSF1A was observed in the SKOV-3 cells transfected with RASSF1A and no expression was observed in the untreated SKOV-3 cells. This finding verifies that SKOV-3 cells do not express RASSF1A and suggests that the transfection efficiency was very high.

Secondly, the morphology, structure, apoptosis and cell cycle progression of SKOV-3 cells before and after transfection with RASSF1A were examined under a fluorescence microscope, TEM and flow cytometer, respectively. Compared with the untreated cells, the transfected SKOV-3 cells were round in shape, their volumes were increased, and the nuclei were vacuolated. In addition, fluorescence was observed in the cytoplasm and was mainly distributed in the cytoskeleton. Moreover, the nuclear chromatin of the transfected cells displayed showed marked shrinkage, condensation and formed apoptotic bodies. All these changes in morphology and structure are in accordance with those observed in a previous study (29). In addition, the apoptosis of the SKOV-3 cells transfected with RASSF1A was significantly higher compared with the other (untreated) cells. Our result indicated that the SKOV-3 cells transfected with adenovirus carrying RASSF1A were mainly located at the S phase of the cell cycle; these results are consistent with those of a previous study reporting that RASSF1A overexpression induces G2/M cell cycle arrest (30). These data indicate that RASSF1A modulates the cell cycle, as was also

Table II. Significant pathways in the RASSF1A-related protein-protein interaction network.

| Term	Description	Count	P-value	Genes
hsa05219	Bladder cancer	4	1.79E-05	HRAS, CDKN2A, RASSF1, MDM2
hsa05223	Non-small cell lung cancer	4	3.85E-05	HRAS, CDKN2A, RASSF1, STK4
hsa05200	Pathways in cancer	5	5.09E-04	HRAS, CDKN2A, RASSF1, MDM2, STK4
hsa05214	Glioma	3	3.05E-03	HRAS, CDKN2A, MDM2
hsa05218	Melanoma	3	3.86E-03	HRAS, CDKN2A, MDM2
hsa05220	Chronic myeloid leukemia	3	4.30E-03	HRAS, CDKN2A, MDM2
hsa04110	Cell cycle	3	1.16E-02	CDKN2A, MDM2, CDC20
hsa04010	MAPK signaling pathway	3	4.84E-02	HRAS, STK4, STK3
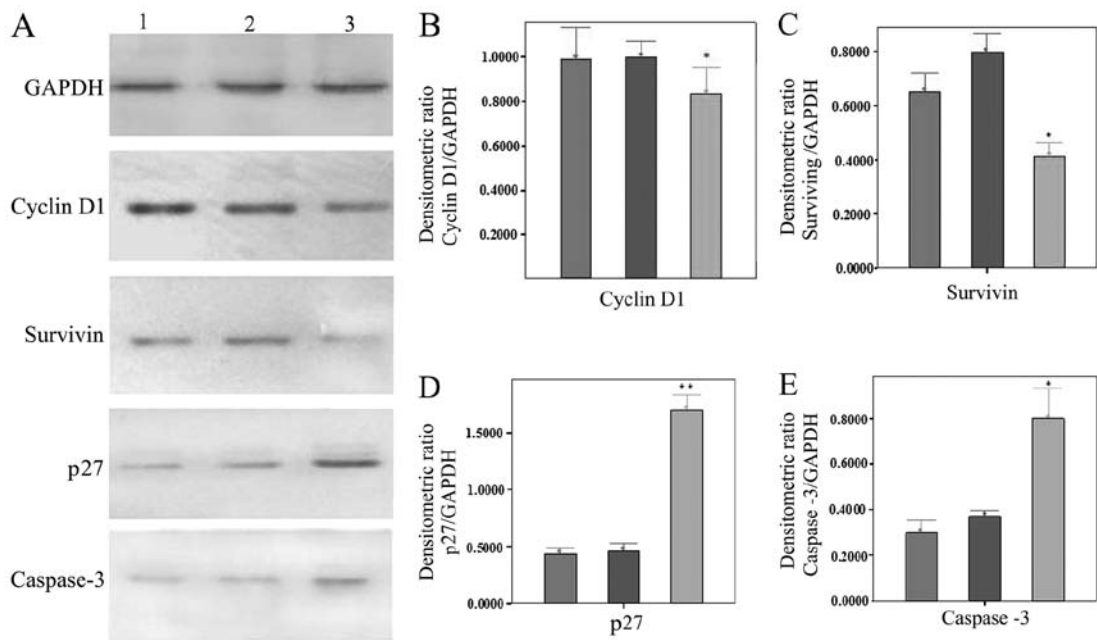
Figure 5. Expression of 4 types of protein in the differently treated SKOV-3 cells. (A) Expression of GAPDH, cyclin D1, survivin, p27 and caspase-3. Lanes 1-3 represent untransfected SKOV-3 cells, those transfected without and those transfected with adenovirus carrying Ras-association domain family 1, isoform A (RASSF1A), respectively. (B-E) Quantification of the results of cyclin D1, survivin, p27 and caspase-3, respectively. $^{*}P<0.05$ and $^{**}P<0.01$, statistically significant differences.
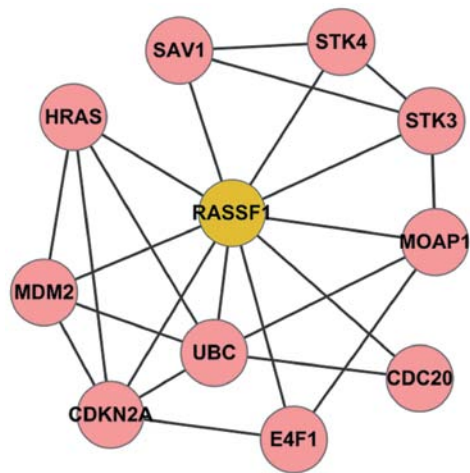

Figure 6. Ras-association domain family 1, isoform A (RASSF1A)-related protein-protein interaction (PPI) network. Yellow circle represents RASSF1A and red circles represent RASSF1A-related genes.

shown in the study by Matallanas *et al* (31), who reported that RASSF1A promotes cell cycle arrest and apoptosis.

In this study, the expression of proliferation-related proteins, including cyclin D1, survivin, p27 and caspase-3 was also examined in the SKOV-3 cells before and after transfection with adenorius with or without RASSF1A by western blot analysis. Cyclin D1 is a component of the core cell cycle machinery and is usually overexpressed in human cancers (32). As a member of the inhibitor of apoptosis protein (IAP) family, survivin is upregulated in almost all human tumors (33). Our results demonstrated that the expression of cyclin D1 and survivin was decreased in the SKOV-3 cells transfected with RASSF1A, which indicates that RASSF1A may promote cancer cell apoptosis. Additionally, the cyclin-dependent kinase (Cdk) inhibitor, p27, regulates cell proliferation, cell motility and apoptosis (34). Caspase-3 is a frequently activated death protease by catalyzing the specific cleavage of several key cellular proteins (35). In this study, the expression of p27 and caspase-3 was increased

in the cells transfected with adenovirus carrying RASSF1A, which suggests that RASSF1A suppresses cell proliferation.

Finally, a bioinformatics approach was applied to explore the mechanisms responsible for the effects of RASSF1A on ovarian cancer cells. Between the ovarian cancer and normal samples, the expression of RASSF1A changed insignificantly. The RASSF1A-related PPI network was constructed containing 10 associated genes, including STK4, STK3, HRAS and CDC20. Moreover, these genes were shown to be enriched in 8 cancer-associated pathways, such as bladder cancer, non-small cell lung cancer and pathways in cancer. The members of STKV, STK3 and STK4 localize to the microtubules and interact with RASSF1A to regulate apoptosis (36). The HRAS gene encodes a protein which is involved primarily in the regulation of cell growth, division and apoptosis (37). It has been previously reported that RASSF1A controls mitotic progression by binding to and inhibiting CDC20, which is an activator of the anaphase-promoting complex (38). Of note, our findings are consistent with those of previous studies which have been mentioned above.

Furthermore, these identified genes were involved in several cancer-related pathways, such as bladder cancer, non-small cell lung cancer and pathways in cancer. These results indicate that RASSF1A and its associated genes may suppress the proliferation and promote the apoptosis of cancer cells by affecting these pathways in the development of bladder cancer, non-small cell lung cancer and ovarian cancer. Kim *et al* (39) identified RASSF1A as a promising prognostic marker in recurrent non-muscle invasive bladder cancer. Senchenko *et al* (13) reported that 3 tumor suppressor genes, RASSF1A, RBSP3 and NPRL2, which were identified in the 3p21.3 region, are involved in the development of several types of cancer, including non-small cell lung cancer. Moreover, RASSF1A has been shown to prevent hypertrophy by disrupting the MAPK signaling pathway in cardiac myocytes (40). Therefore, our findings are consistent with those of previous studies and provide some knowledge of the association between RASSF1A and ovarian cancer.

In conclusion, in this study, the expression of RASSF1A was detected in different ovarian cancer cell lines, and its effects on apoptosis and proliferation were examined. Furthermore, the underlying mechanisms were investigated using a bioinformatics approach. Our data demonstrate that RASSF1A promotes apoptosis and suppresses the proliferation of ovarian cancer cells. Our findings provide a biomarker for the early diagnosis and treatment of ovarian cancer. However, further research is required to verify our findings.

Acknowledgements

References

1. Yap TA, Carden CP and Kaye SB: Beyond chemotherapy: targeted therapies in ovarian cancer. Nat Rev Cancer 9: 167-181, 2009.
2. Buys SS, Partridge E, Black A, *et al*: Effect of screening on ovarian cancer mortality: the prostate, lung, colorectal and ovarian (PLCO) cancer screening randomized controlled trial. JAMA 305: 2295-2303, 2011.
3. Vaughan S, Coward JI, Bast RC JC, *et al*: Rethinking ovarian cancer: recommendations for improving outcomes. Nat Rev Cancer 11: 719-725, 2011.
4. Moore RG, Miller MC, Eklund EE, Lu KH, Bast RC Jr and Lambert-Messerlian G: Serum levels of the ovarian cancer biomarker HE4 are decreased in pregnancy and increase with age. Am J Obstet Gynecol 206: 349. e341-e347, 2012.
5. Nosov V, Su F, Amneus M, *et al*: Validation of serum biomarkers for detection of early-stage ovarian cancer. Am J Obstet Gynecol 200: 639. e631-e635, 2009.
6. Weiland F, Martin K, Oehler MK and Hoffmann P: Deciphering the molecular nature of ovarian cancer biomarker CA125. Int J Mol Sci 13: 10568-10582, 2012.
7. Yee KS, Grochola L, Hamilton G, *et al*: A RASSF1A polymorphism restricts p53/p73 activation and associates with poor survival and accelerated age of onset of soft tissue sarcoma. Cancer Res 72: 2206-2217, 2012.
8. Donninger H, Barnoud T, Nelson N, *et al*: RASSF1A and the rs2073498 cancer associated SNP. Front oncol 1: 54, 2011.
9. Kassler S, Donninger H, Birrer MJ and Clark GJ: RASSF1A and the taxol response in ovarian cancer. Mol Biol Int 2012: 263267, 2012.
10. Liu L, Kron KJ, Pethe VV, *et al*: Association of tissue promoter methylation levels of APC, TGFβ2, HOXD3 and RASSF1A with prostate cancer progression. Int J Cancer 129: 2454-2462, 2011.
11. Brait M, Loyo M, Rosenbaum E, *et al*: Correlation between BRAF mutation and promoter methylation of TIMP3, RARβ2 and RASSF1A in thyroid cancer. Epigenetics 7: 710-719, 2012.
12. Kloten V, Becker B, Winner K, *et al*: Promoter hypermethylation of the tumor-suppressor genes ITIH5, DKK3, and RASSF1A as novel biomarkers for blood-based breast cancer screening. Breast Cancer Res 15: R4, 2013.
13. Senchenko VN, Anedchenko EA, Kondratieva TT, *et al*: Simultaneous down-regulation of tumor suppressor genes RBSP3/CTDSPL, NPRL2/G21 and RASSF1A in primary non-small cell lung cancer. BMC cancer 10: 75, 2010.
14. Yi M, Yang J, Chen X, *et al*: RASSF1A suppresses melanoma development by modulating apoptosis and cell-cycle progression. J Cell Physiol 226: 2360-2369, 2011.
15. Amin KS and Banerjee PP: The cellular functions of RASSF1A and its inactivation in prostate cancer. J Carcinog 11: 3, 2012.
16. Laird PW: Principles and challenges of genomewide DNA methylation analysis. Nat Rev Genet 11: 191-203, 2010.
17. Oh JH, Craft JM, Townsend R, Deasy JO, Bradley JD and El Naqa I: A bioinformatics approach for biomarker identification in radiation-induced lung inflammation from limited proteomics data. J Proteome Res 10: 1406-1415, 2011.
18. Goertsches RH, Zettl UK and Hecker M: Sieving treatment biomarkers from blood gene-expression profiles: a pharmacogenomic update on two types of multiple sclerosis therapy. Pharmacogenomics 12: 423-432, 2011.
19. Kruger NJ: The Bradford method for protein quantitation. In: The Protein Protocols Handbook. Springer, New York, NY, pp17-24, 2009.
20. Chang C, Zhang C, Zhao X, Kuang X, Tang H and Xiao X: Differential regulation of mitogen-activated protein kinase signaling pathways in human with different types of mitral valvular disease. J Surg Res 181: 49-59, 2013.
21. Bowen NJ, Walker LD, Matyunina LV, *et al*: Gene expression profiling supports the hypothesis that human ovarian surface epithelia are multipotent and capable of serving as ovarian cancer initiating cells. BMC Med Genomics 2: 71, 2009.
22. Russell LJ, Capasso M, Vater I, *et al*: Deregulated expression of cytokine receptor gene, CRLF2, is involved in lymphoid transformation in B-cell precursor acute lymphoblastic leukemia. Blood 114: 2688-2698, 2009.
23. Szklarczyk D, Franceschini A, Kuhn M, *et al*: The STRING database in 2011: functional interaction networks of proteins, globally integrated and scored. Nucleic Acids Res 39: D561-D568, 2011.
24. Shannon P, Markiel A, Ozier O, *et al*: Cytoscape: a software environment for integrated models of biomolecular interaction networks. Genome Res 13: 2498-2504, 2003.
25. Huang da W, Sherman BT and Lempicki RA: Systematic and integrative analysis of large gene lists using DAVID bioinformatics resources. Nat Protoc 4: 44-57, 2009.
26. Kanehisa M, Goto S, Furumichi M, Tanabe M and Hirakawa M: KEGG for representation and analysis of molecular networks involving diseases and drugs. Nucleic Acids Res 38: D355-D360, 2010.

27. Kipps E, Tan DS and Kaye SB: Meeting the challenge of ascites in ovarian cancer: new avenues for therapy and research. Nat Rev Cancer 13: 273-282, 2013.
28. Patankar NA, Pritchard J, Van Grinsven M, Osooly M and Bally MB: Topotecan and doxorubicin combination to treat recurrent ovarian cancer: the influence of drug exposure time and delivery systems to achieve optimum therapeutic activity. Clin Cancer Res 19: 865-877, 2013.
29. Pan Y, Du Zhen-Wu D, Zhou JW, et al: MicroRNA-mediated silencing of RhoC inhibits tumor invasion and increases chemo-sensitivity to paclitaxel in SKOV3 cells in vitro. Chem Res Chin Univ 27: 70-74, 2011.
30. Hergovich A and Hemmings BA: Hippo signalling in the G2/M cell cycle phase: lessons learned from the yeast MEN and SIN pathways. Semin Cell Dev Biol 23: 794-802, 2012.
31. Matallanas D, Romano D, Yee K, et al: RASSF1A elicits apoptosis through an MST2 pathway directing proapoptotic transcription by the p73 tumor suppressor protein. Mol Cell 27: 962-975, 2007.
32. Jirawatnotai S, Hu Y, Michowski W, et al: A function for cyclin D1 in DNA repair uncovered by protein interactome analyses in human cancers. Nature 474: 230-234, 2011.
33. Cheung CH, Cheng L, Chang KY, Chen HH and Chang JY: Investigations of survivin: the past, present and future. Front Biosci (Landmark Ed) 16: 952-961, 2010.
34. Chu IM, Hengst L and Slingerland JM: The Cdk inhibitor p27 in human cancer: prognostic potential and relevance to anticancer therapy. Nat Rev Cancer 8: 253-267, 2008.
35. Larsen BD, Rampalli S, Burns LE, Brunette S, Dilworth FJ and Megeney LA: Caspase 3/caspase-activated DNase promote cell differentiation by inducing DNA strand breaks. Proc Natl Acad Sci USA 107: 4230-4235, 2010.
36. Bennani-Baiti IM: Epigenetic and epigenomic mechanisms shape sarcoma and other mesenchymal tumor pathogenesis. Epigenomics 3: 715-732, 2011.
37. Sun XF, Li L, Li XJ and Shen W: Methylation pattern of oncogene HRAS gene promoter region and its clinical relevance to urocystic tumorigenesis. Mol Biol Rep 39: 8431-8437, 2012.
38. Liu L, Baier K, Dammann RH and Pfeifer GP: The tumor suppressor RASSF1A does not interact with Cdc20, an activator of the anaphase-promoting complex. Cell Cycle 6: 1663-1665, 2007.
39. Kim JS, Chae Y, Ha YS, et al: Ras association domain family 1A: a promising prognostic marker in recurrent nonmuscle invasive bladder cancer. Clin Genitourin Cancer 10: 114-120, 2012.
40. Del Re DP and Sadoshima J: RASSF1A Signaling in the heart: novel functions beyond tumor suppression. Mol Biol Int 2012: 154283, 2012.